

This work was written as part of one of the author's official duties as an Employee of the United States Government and is therefore a work of the United States Government. In accordance with 17 U.S.C. 105, no copyright protection is available for such works under U.S. Law.

Public Domain Mark 1.0

<https://creativecommons.org/publicdomain/mark/1.0/>

Access to this work was provided by the University of Maryland, Baltimore County (UMBC) ScholarWorks@UMBC digital repository on the Maryland Shared Open Access (MD-SOAR) platform.

Please provide feedback

Please support the ScholarWorks@UMBC repository by emailing scholarworks-group@umbc.edu and telling us what having access to this work means to you and why it's important to you. Thank you.



Multi-spacecraft investigation of space turbulence: Lessons from Cluster and input to the Cross-Scale mission

Fouad Sahraoui^{a,b,*}, Melvyn L. Goldstein^a, Gérard Belmont^b, Alain Roux^b, Laurence Rezeau^{b,c}, Patrick Canu^b, Patrick Robert^b, Nicole Cornilleau-Wehrin^b, Olivier Le Contel^b, Thierry Dudok De Wit^d, Jean-louis Pinçon^d, Khurom Kiyani^e

^a NASA Goddard Space Flight Center, Code 673, Greenbelt, MD 20771, USA

^b Laboratoire de Physique des Plasmas, CNRS-Ecole Polytechnique, 10-12 Avenue de l'Europe, Vélizy 78140, France

^c Université Pierre et Marie Curie, Place Jussieu, Paris, France

^d Laboratoire de Physique et de Chimie de l'Environnement et de L'espace, LPC2E-CNRS, Université d'Orléans, France

^e Centre for Fusion, Space and Astrophysics, University of Warwick, Coventry CV4 7AL, UK

ARTICLE INFO

Available online 8 June 2010

Keywords:

Cluster
Turbulence
Cross-Scale
k-Filtering
Solar wind
Dissipation

ABSTRACT

Investigating space plasma turbulence from single-point measurements is known to be characterized by unavoidable ambiguities in disentangling temporal and spatial variations. Solving this problem has been one of the major goals of the Cluster mission. For that purpose multipoint measurements techniques, such as the *k*-filtering, have been developed. Such techniques combine several time series recorded simultaneously at different points in space to estimate the corresponding energy density in the wavenumber space. Here we apply the technique to both simulated and Cluster magnetometer data in the solar wind (SW) and investigate the errors and limitations that arise due to the separation of the spacecraft and the quality of the tetrahedral configuration. Specifically, we provide an estimation of the minimum and maximum scales that can be accurately measured given a specific distance between the satellites and show the importance of the geometry of the tetrahedron and the relationship of that geometry to spatial aliasing. We also present recent results on characterizing small scale SW turbulence and provide scientific arguments supporting the need of new magnetometers having better sensitivity than the existing ones. Throughout the paper we emphasize technical challenges and their solutions that can be considered for a better preparation of the Cross-Scale mission.

© 2010 Elsevier Ltd. All rights reserved.

1. Introduction

Since its launch in 2000, the Cluster mission (Escoubet, 1997) has led to significant achievements in understanding space plasma turbulence, in particular in revealing new 3-D properties of turbulence using multipoint measurement techniques such as *k*-filtering (Glassmeier et al., 2001; Sahraoui et al., 2003, 2004; Constantinescu et al., 2006; Narita et al., 2006). The *k*-filtering method combines several time series recorded simultaneously at different points in space to estimate in Fourier space the four-dimensional (4-D) function $P(\omega, \mathbf{k})$ (Pinçon and Lefeuvre, 1988, 1991, 1992; Neubauer and Glassmeier, 1990). The method requires the time series to be sufficiently time stationary and spatially homogeneous. We emphasize that the *k*-filtering does not assume any physics about the data under study, such as an

existing linear dispersion relation or the weak (or strong) nature of nonlinearities at work. In this sense it is the most general existing method applicable to space turbulence. The method allows one to include additional theoretical constraints, such as the divergence-free equation $\nabla \cdot \delta \mathbf{B} = 0$ for magnetic field fluctuations. The quantity $P(\omega, \mathbf{k})$ has been used to obtain 3-D experimental dispersion relations of low frequency plasma modes from the magnetic field data in the magnetosheath (Glassmeier et al., 2001; Sahraoui et al., 2003, 2004) and in the cusp region (Grison et al., 2005). It has also been applied to both electric and magnetic field data for the same purpose (Tjulin et al., 2005). For turbulence studies, Sahraoui et al. (2006) have used *k*-filtering to compute the first 3-D wavenumber spectrum of low frequency magnetosheath turbulence $P(\mathbf{k})$ by integrating over the angular frequencies: $P(\mathbf{k}) = \int P(\omega, \mathbf{k}) d\omega$.

In this paper we apply the technique to both simulated and Cluster magnetometer data in the solar wind to investigate some technical problems such as the accuracy of the wavenumber estimation and spatial aliasing. In Section 2 we discuss how the wavenumber space is defined given an average spacecraft

* Corresponding author at: Laboratoire de Physique des Plasmas, CNRS-Ecole Polytechnique, Observatoire de Saint-Maur, 4 avenue de Neptune, 94107 Saint-Maur-Des-Fossés, France. Tel.: +33 1 39 25 49 40.

E-mail address: fouad.sahraoui@lpp.polytechnique.fr (F. Sahraoui).

separation. Based on uncertainty estimations of the wavenumber we provide an estimate of the separation required for the Cross-Scale satellites to ensure full coverage of three different ranges of scales. In Section 3 we will show the importance of the tetrahedron shape of the Cluster spacecraft and its dramatic impact on the accuracy of the wavenumber estimation. In Section 4 we show recent results on small scale solar turbulence and emphasize limitations imposed by the sensitivity of the existing instruments. We provide scientific arguments justifying the need to develop new magnetometers with improved sensitivity and suggest that these new requirements be considered in preparing the Cross-Scale mission.

2. Appropriate separations for the Cross-Scale satellites: k -filtering analysis

Based on analogy with temporal Fourier transform, the k -filtering technique assumes that, if d is the average separation between the spacecraft, then all the wavelengths present within the data belong to $[-k_{\max}, k_{\max}]$, where $k_{\max} = \pi/d$. If wavelengths smaller than $2d$ exist in the data and propagate undamped past the satellites, aliasing will occur and consequently spurious energy peaks will appear in the wavenumber domain $[-k_{\max}, k_{\max}]$ (Pinçon and Motschmann, 1998; Sahraoui et al., 2003). Technically there is no direct way to filter wavenumbers larger than k_{\max} (in temporal Fourier analyzes an anti-aliasing filter is implemented into the experiment). Fortunately, since the measured frequency is generally an increasing function of the wavenumber (either when a dispersion relation exists or the Taylor assumption is valid), one can show that this problem can be avoided—or limited—by restricting the investigated frequencies to some range $[-\omega_{\max}, \omega_{\max}]$. To define these limit, consider a medium with a flow speed V_f and a maximum phase speed of waves $V_{\phi_{\max}}$. This implies that all the existing waves have propagation velocities V_{sc} in the spacecraft frame that belong to a range $V_f - V_{\phi_{\max}} < V_{sc} < V_f + V_{\phi_{\max}}$. Therefore, provided that $V_{\phi_{\max}}$ had been accurately estimated, to avoid spatial aliasing one must limit the investigated frequencies (in the spacecraft reference frame) to $\omega_{\max} = k_{\max}(V_f - V_{\phi_{\max}})$.

Now what is the smallest k -vector k_{\min} (or equivalently, the largest scale) that can be measured accurately given the separation d ? The answer to this question is linked to the definition of the highest possible resolution δk of the k -space to consider. One possible solution would be to infer δk from $\delta k \sim \delta \omega / V_f$, where $\delta \omega = 2\pi/T$ is the resolution of the temporal spectra calculated over the time interval T . However, this estimation suffers from the weakness that it is independent of the spacecraft separation d . And yet one would expect that, given a separation d , the scale $L \sim d$, for instance, will be resolved with a better accuracy than $L \sim 10d$ or $L \sim 100d$ (as we will show below). The estimation of the largest scale can thus be determined only empirically through uncertainty estimation of the k -vectors.

We performed a set of numerical simulations to quantify those uncertainties by generating a set of monochromatic waves $\exp[-i(\omega_0 t + \mathbf{k}_s \cdot \mathbf{r})]$, where ω_0 is fixed and the wave vectors \mathbf{k}_s range from $0.01k_{\max}$ to k_{\max} . Then we applied the k -filtering technique to detect such waves and measure their wave vectors \mathbf{k}_{mes} . The errors $\Delta k = |\mathbf{k}_s - \mathbf{k}_{mes}|$ were then computed and found to range from δk to $4\delta k$ (where $\delta k = 0.0001$ rd/km is the adopted resolution). Consequently, the actual resolution is, at best, ~ 0.0004 rd/km, which is four time larger than the one used. Fig. 1 shows that the relative errors $\Delta k_s/k_s$ remains very small for scales of the order of the spacecraft separation d or larger up to about a decade. But then errors increase significantly for larger scales and reach 100% at scales $\sim 100d$. Therefore, one can say

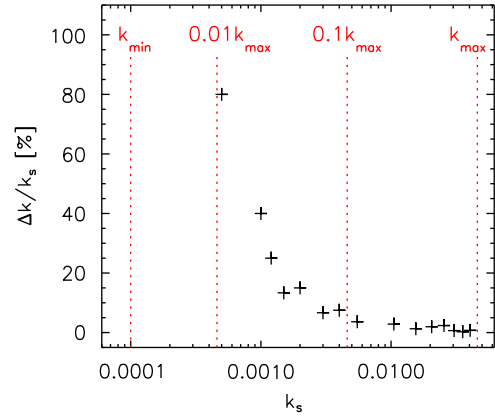


Fig. 1. Relative errors in the determination of the wave vector \mathbf{k}_s of the simulated plane waves. \mathbf{k}_s is chosen to vary from $[0.01k_{\max}, k_{\max}]$. $k_{\max} \sim \pi/d$ and $k_{\min} = \delta k = 0.0001$ rd/km is the chosen resolution of the k -space.

that given a separation d of the Cluster spacecraft the scales that can be resolved within reasonable errors bars ($< 10\%$) are, at most, one and a half decades beyond the spacecraft separation d . We recall that other sources of uncertainties (not considered here) may come from the spacecraft positions, the change of the separations and/or the shape of the Cluster tetrahedron over long intervals of time (\sim a few hours). This would occur for instance if one were to investigate large-scale SW turbulence, where such long data intervals are required.

The smallest accessible k -vector defined above yields the smallest frequency to analyze $\omega_{\min} = k_{\min}(V_f - V_{\phi_{\max}})$. Fig. 2 shows estimations of the limits ω_{\max} and ω_{\min} in two cases of SW data with two different Cluster separations. In day 2006-02-14 (Fig. 2) the spacecraft were separated by $\sim 4 \times 10^3$ km and the flow speed $V_f \sim 340$ km/s, whereas for day 2004-01-10 the separation were $\sim 2 \times 10^2$ km and the flow speed $V_f \sim 540$ km/s. These examples show clearly that, for a given separation, only one range of scales can be resolved properly.

This provides a strong constraint on the spacecraft separations needed for the Cross-Scale mission. For turbulence studies, if the separations of the inner four satellites is set to 10 km, the medium and outer satellites need to be separated, respectively, by less than 500 and 10000 km. We emphasize that each quartet of satellites will resolve only one range of scales at once. If each quartet is far away from the others then using all the twelve satellites (in the optimal case) does not provide a better accuracy than with four. For instance, if the outer four satellites are separated by a distance $D \sim 5000$ km, considering data from an inner satellite separated by a $d \sim 10$ km from the outer quartet will produce higher uncertainty on scales of 10000 km than if it were computed from the outer quartet alone (Pinçon and Lefeuvre, 1992). In order for Cross-Scale to provide a better accuracy in the wavenumber determination than the present one available with Cluster it is necessary to have more than four satellites at comparable separations.

3. The tetrahedral configuration of the spacecraft and the k -spectra of the turbulence

The tetrahedron formed by the four Cluster spacecraft may change dramatically along a given orbit. The shape of the tetrahedron is controlled by two parameters, namely the elongation E and the planarity P . $E \sim P \sim 0$ reflects a regular tetrahedron, while $P \sim 1$ and $E \sim 1$ reflect, respectively, a “cigar” and a “pancake” shape (Robert et al., 1998). It is obvious that for the

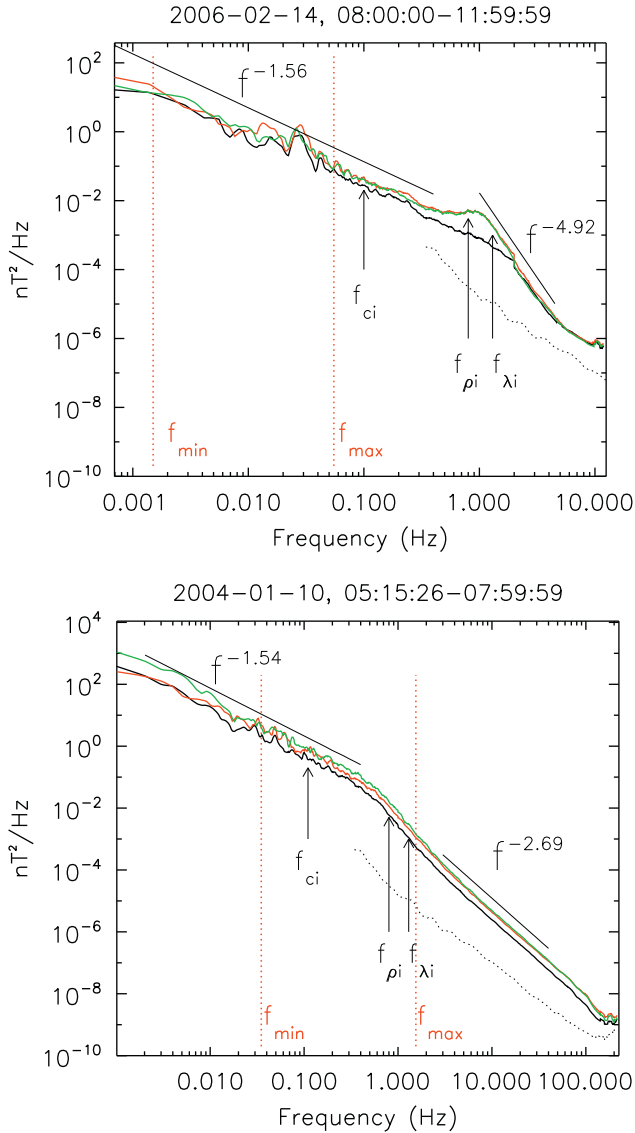


Fig. 2. Power spectra measured in the SW by FGM (< 1.5 Hz) and STAFF-SC (> 1.5 Hz): B_x (black), B_y (red) and B_z (green). The spacecraft separation were 4×10^3 km (day 2006-02-14) and 200 km (day 2004-01-10). The vertical dotted lines delimit the estimated range of frequencies to which the k -filtering can be applied (see text). The vertical arrows are the ion gyrofrequency f_{ci} and the Doppler-shifted ion inertial length $f_{\lambda_i} = V_f/2\pi\lambda_i$ and ion gyroscale $f_{\rho_i} = V_f/2\pi\rho_i$. (For interpretation of the references to color in this figure legend, the reader is referred to the web version of this article.)

purpose of determining the 3-D properties of the turbulence, a regular tetrahedron is desired. Unfortunately, this requirement has often been ignored. Here we demonstrate just how misleading the k -spectra obtained from Cluster data can be when the geometry of the tetrahedron is inappropriate.

Consider the magnetic field spectra shown in Fig. 2. They were recorded in the SW by the FGM and STAFF-SC magnetometers on spacecraft 2 (Balogh et al., 2001; Cornilleau-Wehrlin et al., 2003). Because FGM data are noisy above 2 Hz (Sahraoui et al., 2009), frequencies above > 1.5 Hz are computed using the STAFF data, which has a better sensitivity at high frequencies (Cornilleau-Wehrlin et al., 2003). The spectra in Fig. 2 show a similar Kolmogorov-like scaling $f^{-5/3}$ for $f < 0.4$ Hz, generally referred to as the inertial range of Alfvénic turbulence. Around the Doppler shifted ion gyroscale or inertial length (~ 1 Hz) a break

point or a bump is observed. Below that frequency the two spectra show, however, different physics: a “dissipation”-like scaling $f^{-4.9}$ for $f > 1$ Hz (day 2006-02-14) (Goldstein et al., 1994; Leamon et al., 1998) and a second dispersive inertial range with a scaling $f^{-2.7}$ (day 2004-01-10) (Sahraoui et al., 2009; Kiyani et al., 2009; Alexandrova et al., 2009). We defer further discussion of the physics of the inertial and dissipation ranges for these time intervals to a forthcoming paper.

Let us therefore resume our discussion on the use of the k -filtering technique. The spacecraft separation were different in the chosen events: $d \sim 4 \times 10^3$ km (day 2006-02-14) and ~ 200 km (day 2004-01-10). These separations yield estimated maximum wave vectors to analyze using the k -filtering $k_{\max} \sim 10^{-3}$ rd/km and 2×10^{-2} rd/km. Furthermore, using the flow speeds given above, we obtain the frequency intervals that we can analyze accurately using the k -filtering (estimated from Section 2) $[f_{\min}, f_{\max}] \sim [0.002, 0.05]$ Hz and $[0.03, 1.5]$ Hz. These frequency limits are shown on Fig. 2. It is important to note that these limits cover different inertial ranges of the spectra: the classical Kolmogorov inertial zone (day 2006-02-14) and the zone of transition to the dispersive inertial range (day 2004-01-10). We cannot address both ranges of scales simultaneously as explained above. Application of the k -filtering to the frequency $f = 0.03$ Hz taken from the interval $[f_{\min}, f_{\max}]$ of Fig. 2 (day 2006-02-14) yields the k -spectra shown in Fig. 3. The maximum of the energy is centered around the wave vector $\mathbf{k}_0 = (-32, -31, 32) \times 10^{-5}$ rd/km. The most striking aspect of Fig. 3 is the stretching of the k -spectra in a particular direction in each plane. Is the “anisotropy” physical? Does the high SW speed play any role in generating this anisotropy as may be suggested by the near alignment of the projection of the flow speed onto the planes (k_x, k_y) and (k_x, k_z) ? Before answering these questions, we note first that the orientation of the energy density does not follow the blue curve $\omega_{sc} = \mathbf{k} \cdot \mathbf{V}_f$ (or $\omega_f = 0$), which is expected to govern Alfvénic turbulence generally observed at these frequencies in the SW (since $V_A \ll V_f$) or mirror mode turbulence in the magnetosheath Sahraoui et al. (2003, 2006).

Indeed, applying the k -filtering to the frequency 0.12 Hz of the spectrum of Fig. 2 (day 2004-01-10) shows that the energy is rather well localized in k -space and lies very close to the curve $\omega_{sc} = \mathbf{k} \cdot \mathbf{V}_f$, as one would expect.

To explain the source of anisotropy in Fig. 3, we consider a new simulation using a plane wave with the same wave vector $\mathbf{k} = \mathbf{k}_0$ and the same Cluster tetrahedron as is observed in the real data. In this simulation we do not use any flow speed, neither do we introduce any Doppler shift. The simulated wave propagates past the satellites with a phase speed $V_\phi = \omega_0/|\mathbf{k}_0|$, where ω_0 is the angular frequency of the wave. The results are shown on Fig. 5. It is remarkable to see how these simulated results reproduce the anisotropies observed in the real data. We can now state that the observed anisotropy in the real data is an artifact caused largely by the shape of the Cluster tetrahedron. In Fig. 5 we have overplotted the projection of the spacecraft positions (re-scaled to the size of the k -cell). The projection shows that the satellites are strongly elongated along a direction in the (X_{GSE}, Z_{GSE}) that is perpendicular to the direction of the anisotropy. This stretching is also present in the two other planes, although it is less pronounced. This means that the spacecraft are far from forming a regular tetrahedron. In fact, the shape is nearly all in the (Y_{GSE}, Z_{GSE}) plane and is slightly elongated in that plane, as it is confirmed by the planarity and the elongation parameters, $P \sim 0.8$ and $E \sim 0.6$. The main shortcoming of the Cluster geometry at this time is that the direction perpendicular to the “pancake” or to the “cigar” is under-sampled and that leads to large uncertainties in estimating the wavenumber spectra in that direction. The uncertainties are smaller (i.e., the energy peaks are less stretched)

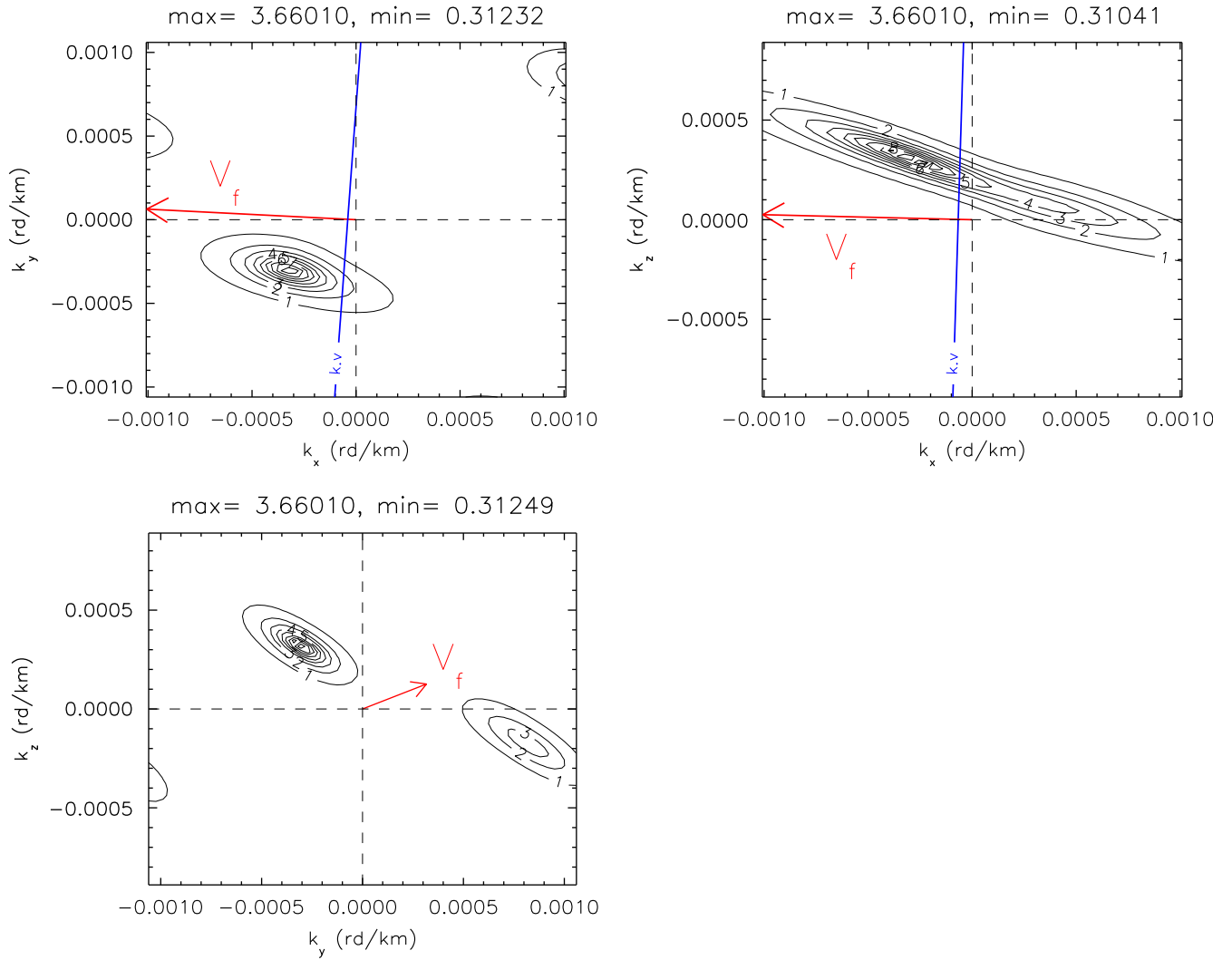


Fig. 3. Wavenumber spectra for the frequency $f=0.03$ Hz from Fig. 2 (day 2006-02-14) represented in the three planes of the \mathbf{k} -space. The blue line is the solution of the equation $\omega_{sc} = \mathbf{k} \cdot \mathbf{V}_f$. The red arrows are the projections of the flow speed on each plane (the component in the plane (k_y, k_z) is magnified by a factor 5 for the clarity of the plot). (For interpretation of the references to color in this figure legend, the reader is referred to the web version of this article.)

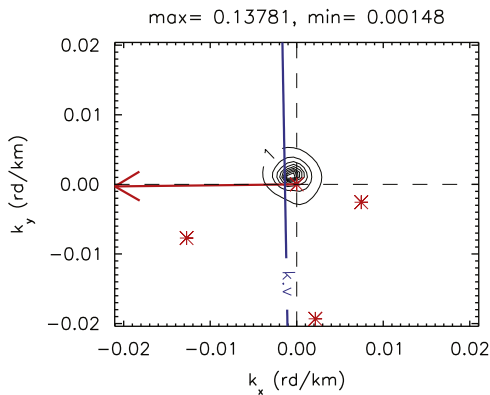


Fig. 4. Wavenumber spectra for the frequency $f=0.12$ Hz from the spectrum of Fig. 2 (day 2004-01-10) in the plane (k_x, k_y) . The red crosses are the projections of spacecraft positions on each plane (re-scaled to the size of the k -cell). (For interpretation of the references to color in this figure legend, the reader is referred to the web version of this article.)

when the spatial coverage is better as in Fig. 4. This example illustrates how misleading the k -filtering results can be when all the conditions of its applicability are not fulfilled.

We emphasize here that this effect is different from the aliasing effect discussed previously. It concerns the large uncertainty in the k -vector determination due to an inadequate spatial sampling. The aliasing effect may additionally come into play and further distort the k -spectra. This is illustrated in Fig. 6, where a spurious peak appears in the fundamental k -cell at exactly the same wavenumber $\mathbf{k}_0 = (5.5, -9) \times 10^{-4}$ rd/km for both the simulated plane wave and the real data. We note finally that adding electric field data to the analysis may help to reduce aliasing by imposing an additional theoretical constraint, viz., Faraday's law, on the measured \mathbf{k} -vectors (Tjulin et al., 2005). But this does not fundamentally change the problem: aliasing cannot be suppressed totally. Only satisfying all the requirements that we have discussed above will lead to meaningful results that are minimally affected by aliasing.

4. Small scale solar wind turbulence and the sensitivity of the magnetometers

Besides the unique opportunity offered by Cluster to determine 3-D properties of turbulence, its high resolution wave data has led to making significant progress in understanding small scale turbulence in the magnetosphere and, more recently, in the SW (Sahraoui et al., 2009; Kiyani et al., 2009; Alexandrova et al.,

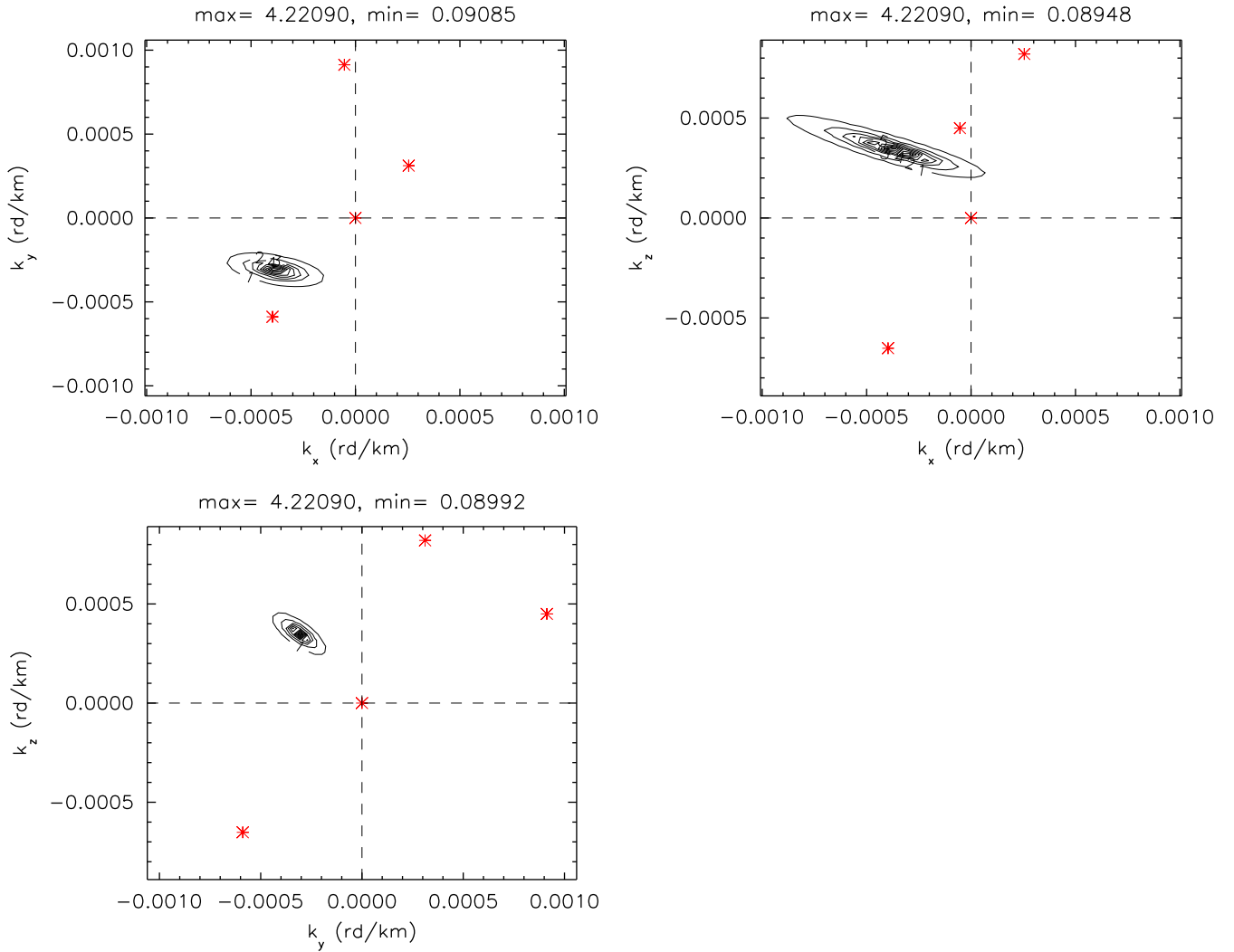


Fig. 5. k -spectra for a simulated plane with $k = (-32, -31, 32) \times 10^{-5}$ rd/km in the three planes of the k -space calculated using the same tetrahedron as in the real data. The red crosses are the projections of spacecraft positions on each plane (re-scaled to the size of the k -cell). (For interpretation of the references to color in this figure legend, the reader is referred to the web version of this article.)

2009). Indeed, one of the hot topics that is being currently investigated using the Cluster data is the determination of the nature of small-scale SW turbulence (i.e., above the proton gyrofrequency). A long standing question to answer is whether, or more specifically, under which conditions the turbulence dissipates at the proton scales (Leamon et al., 1998) or continues the cascade down to electrons scales (Bale et al., 2005). Furthermore, if a cascade down to electron scales occurs then which plasma mode can carry such a cascade: Kinetic Alfvén Wave (KAW) or whistler mode (Gary and Smith, 2009)? Using STAFF-SC and burst mode data (up to ~ 100 Hz) Sahraoui et al. (2009) have shown for the first time a clear evidence that large scale SW turbulence cascades down to the electron gyroscale where it is dissipated via electron Landau damping. Moreover, this was shown to be carried by KAW turbulence. Alexandrova et al. (2009) confirmed in a few more cases the same processes of cascade and dissipation at electrons scales (without analyzing the KAW or whistler nature of the turbulence). Kiyani et al. (2009) have analyzed the statistical properties of the turbulence and found an unexpected global scale invariance of the turbulence at sub-proton scales, which contrasts with multi-fractality usually observed in the Kolmogorov-like inertial range.

However, those results have unveiled strong limitations imposed by the sensitivity of the Search-Coil magnetometers

(SCM). Fig. 7 shows indeed that, in some instances (e.g., day 2007-01-20), high frequency SW turbulence exhibits low levels of magnetic fluctuations that are barely above the sensitivity level of the SCM for $f > 10$ Hz. This strongly limits the possibilities of studying properly the turbulence at electron scales.

This can be seen more clearly on Fig. 8 which compares the ratios of the spectra of Fig. 7 to the sensitivity floor of the SCM as estimated from data measured in the lobes. For the sake of simplicity, we refer to these ratios as Signal to Noise Ratios (SNRs), although sensitivity as measured in the lobes does not necessarily reflect the electronic noise of the instrument, which has an even lower level. The SNR is defined as $\log_{10}(\delta B^2 / \delta B_{sens}^2)$, where δB is the measured power spectrum in the SW and δB_{sens} is the sensitivity curve of the SCM as measured in the lobes. If one defines an interval of confidence as where $SNR > 5$, then one can see that this threshold is reached at frequencies varying from 5 Hz to ~ 100 Hz, which are below the electron gyrofrequency f_{ce} (Fig. 8). This limitation does not allow us, for instance, to address properly high frequency whistler turbulence. It is important to notice that choosing data when the SNR is high does not necessarily enable solving this problem because higher SNR means also strong B , and consequently, higher values of f_{ce} (and smaller electron scales for a constant temperature). We emphasize that this limitation applies to STAFF-SA data as

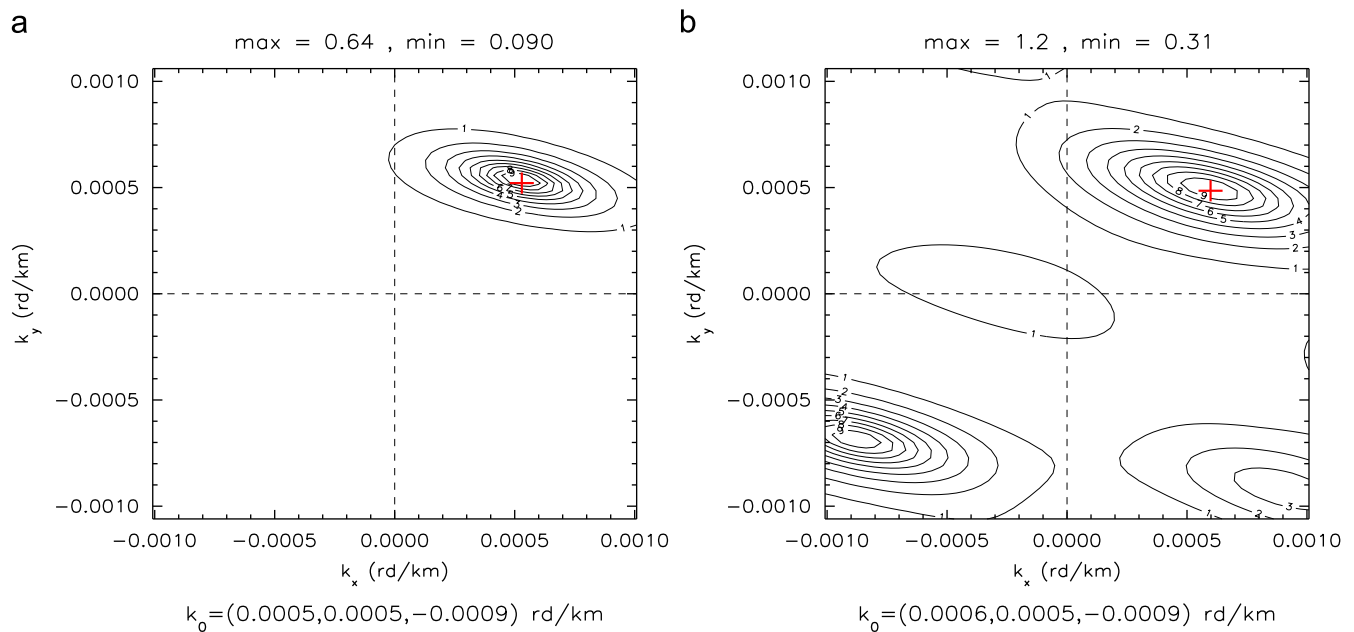


Fig. 6. Evidence of an aliased energy peak at the same location (red cross) for the simulated plane wave (a) and the real data (b). (For interpretation of the references to color in this figure legend, the reader is referred to the web version of this article.)

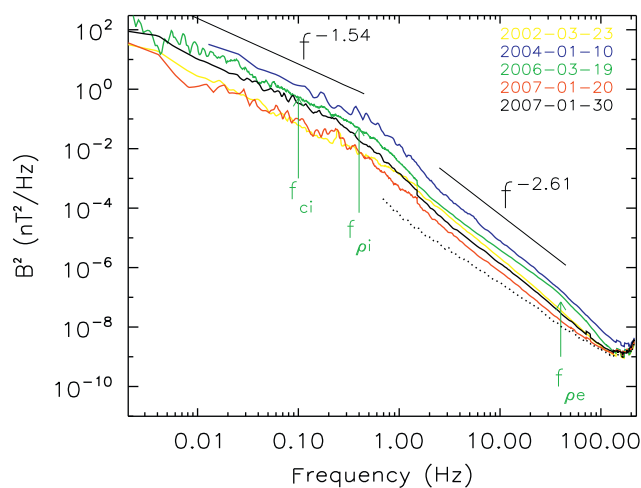


Fig. 7. Power spectra from FGM and STAFF-SC data (merged at 1.5 Hz) measured onboard spacecraft 2 in the free-solar wind (Whisper data were used to locate periods of time without connection to the bow shock). The dotted line is the sensitivity curve of the spacecraft as estimated from data measured in the lobes on 2007-06-30, from 15h00 to 15h20.

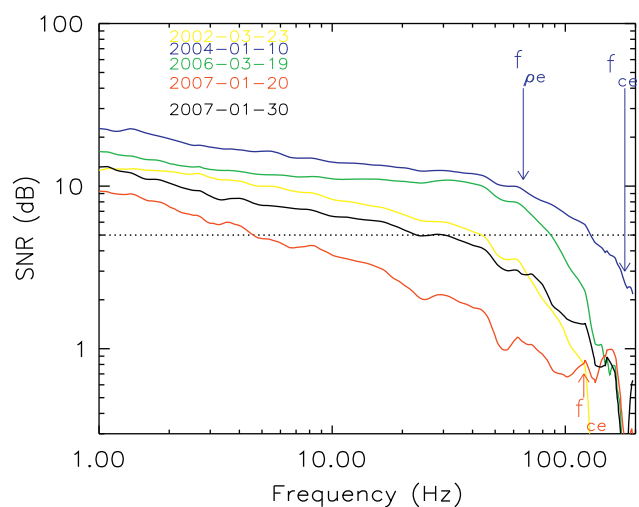


Fig. 8. SNRs for the same spectra as in Fig. 7. The horizontal dotted line is the value $SNR=5$ dB. Vertical arrows show typical electron scales/frequencies for the days with the highest and lowest SNRs.

well, as one can see in Fig. 8 where for frequencies $\sim f_{ce}$ we found $SNR \sim 1$.

Nevertheless, when the level of the turbulence is significantly high (e.g., days 2006-03-19 on STAFF-SC or 2004-01-22 on STAFF-SA) it is possible to address the physics occurring at electron spatial scales ρ_e or d_e if the Taylor hypothesis (known also as the frozen-in-flow approximation $\omega \sim \mathbf{k} \cdot \mathbf{V}_f$) is valid. This requires that all phase speeds of the fluctuations are smaller than the flow speed V_f , a condition that can be fulfilled by the KAW turbulence (as reported in Sahraoui et al., 2009) but not by the whistler turbulence. In this particular case Doppler-shifting the scales ρ_e or d_e results indeed in frequencies $f_{\rho_e} \sim V_f/2\pi\rho_e$ and $f_{d_e} \sim V_f/2\pi d_e$ that fall above the threshold $SNR=5$ as shown on Figs. 8 and 9. Note, however, that even in these instances, resolving unambiguously the actual scaling of the dissipation range that forms below the electron scales is not

possible. The reason is that the dissipation range extends over a short range of scales (less than a decade) before hitting the noise floor. Whether the scaling is a power law (Sahraoui et al., 2009), an exponential (Alexandrova et al., 2009) or a cut-off is still an open question, that cannot be addressed unambiguously by the Cluster data. Therefore, it is necessary for future missions to have more sensitive magnetometers than the present ones. From Figs. 7 to 9, it appears that improving the sensitivity by, at least, a factor 10 for the Cross-Scale mission is necessary in order to solve the challenging problem of dissipation at electron scales in the SW. Typically, this would require to target a sensitivity level better than 10^{-5} nT/ $\sqrt{\text{Hz}}$ at 100 Hz (as compared to 4×10^{-5} nT/ $\sqrt{\text{Hz}}$ on Cluster). We note finally that problems of noise related to high frequency Cluster electric field data in the SW have been also reported in Sahraoui et al. (2009).

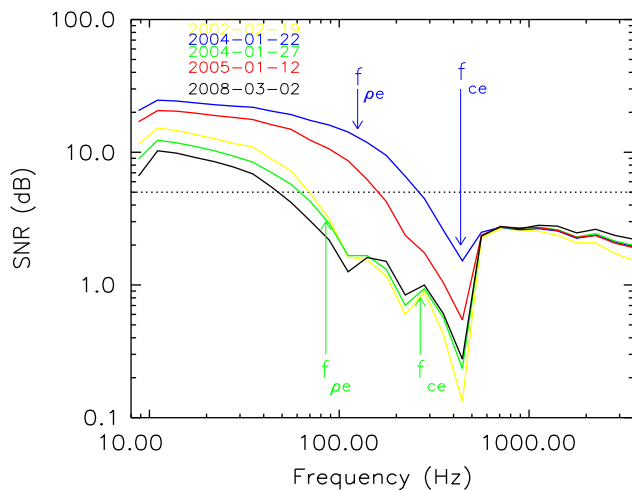


Fig. 9. SNRs of power spectra measured by the STAFF-SA instrument in the SW (some of these data were studied in Alexandrova et al., 2009). The same description as in Fig. 8 applies.

5. Conclusions

With the k -filtering technique as applied to both simulated and Cluster SW data we have provided estimations of the separation distances appropriate for the Cross-Scale satellites. Estimation of wave number spectra of turbulence at three different scales requires separations of 10, 500 and 5000 km. For each quartet, resolving scales larger by more than one decade above the average separation is subject to significant uncertainties. We have shown the importance of achieving a regular tetrahedron of the spacecraft, otherwise distorted wave number spectra of the turbulence and aliasing effects will occur. We have also shown from several examples of spectra of small scale SW turbulence the necessity of developing magnetometers with better sensitivity, typically 10^{-5} nT/ $\sqrt{\text{Hz}}$ at 100 Hz. This point is crucial for solving the problem of the dissipation and heating of SW turbulence. Finally, it is worth keeping in mind that at 1 AU the characteristic fields are lower than they are in the inner heliosphere and corona. Thus, measurements at 1 AU may be better suited to studying the processes that heat the corona than are measurements in the corona despite the higher signal levels expected to be present in the inner heliosphere.

References

- Alexandrova, O., Saur, J., Lacombe, C., Mangeney, A., Mitchell, J., Schwartz, S.J., Robert, P., 2009. Universality of solar-wind turbulent spectrum from MHD to electron scales. *Phys. Rev. Lett.* 103, 165003.
- Bale, S.D., Kellogg, P.J., Mozer, F.S., Horbury, T.S., Rème, H., 2005. Observations of turbulence generated by magnetic reconnection. *Phys. Rev. Lett.* 94, 215002.

- Balogh, A., Carr, C.M., Acuna, M.H., Dunlop, M.W., Beek, T.J., Brown, P., Fornacon, K.-H., Georgescu, E., Glassmeier, K.-H., Harris, J., Musmann, G., Oddy, T., Schwingenschuh, K., 2001. The cluster magnetic field investigation: overview of in-flight performance and initial results. *Ann. Geophys.* 19, 1207–1217.
- Constantinescu, O.D., Glassmeier, K.-H., Motschmann, U., Treumann, R.A., Fornacon, K.-H., Franz, M., 2006. Plasma wave source location using CLUSTER as a spherical wave telescope. *J. Geophys. Res.* 111, A09221.
- Cornilleau-Wehrin, N., Chanteur, G., Perraut, S., Rezeau, L., Robert, P., Roux, A., de Villedary, C., Canu, P., Maksimovic, M., de Conchy, Y., Hubert, D., Lacombe, C., Lefeuvre, F., Parrot, M., Pinçon, J.L., Décréau, P.M.E., Harvey, C.C., Louarn, Ph., Santolik, O., Alleyne, H.St.C., Roth, M., Chust, T., Le Contel, O., 2003. STAFF Team, 2003. First results obtained by the Cluster STAFF experiment. *Ann. Geophys.* 21, 437–456.
- Escoubet, P., et al., 1997. The Cluster and Phoenix Missions. Kluwer Academic Publishers, Belgium.
- Gary, S.P., Smith, C.W., 2009. Short-wavelength turbulence in the solar wind: linear theory of whistler and kinetic Alfvén fluctuations. *J. Geophys. Res.* 114, A12105, doi:10.1029/2009JA014525, 2009.
- Glassmeier, K.-H., Motschmann, U., Dunlop, M., Balogh, A., Acuna, M.H., Carr, C., Musmann, G., Fornacon, K.-H., Schweda, K., Vogt, J., Georgescu, E., Buchert, S., 2001. *Ann. Geophys.* 19, 1439–1447.
- Goldstein, M.L., Roberts, M.D., Fitch, C., 1994. Properties of the fluctuating magnetic helicity in the inertial and dissipation ranges of solar wind turbulence. *J. Geophys. Res.* 99, 11519–11538.
- Grisson, B., Sahraoui, F., Lavraud, B., Chust, T., Cornilleau-Wehrin, N., Rème, H., Balogh, A., André, M., 2005. Wave particle interactions in the high-altitude polar cusp: a Cluster case study. *Ann. Geophys.* 23, 3699–3713.
- Kiyani, K.H., Chapman, S.C., Khotyaintsev, Y.V., Dunlop, M.W., Sahraoui, F., 2009. Global scale-invariant dissipation in collisionless plasma turbulence. *Phys. Rev. Lett.* 103, 075006.
- Leamon, R.J., Smith, C.W., Ness, N.F., Matthaeus, W.H., Wong, H.K., 1998. Observational constraints on the dynamics of the interplanetary magnetic field dissipation range. *J. Geophys. Res.* 103, 4775–4787.
- Narita, Y., Glassmeier, K.-H., Treumann, R.A., 2006. Wave-number spectra and intermittency in the terrestrial foreshock region. *Phys. Rev. Lett.* 97, 191101.
- Neubauer, F.M., Glassmeier, K.H., 1990. Use of an array of satellite as a wave telescope. *J. Geophys. Res.* 95, 19115–19122.
- Pinçon, J.L., Lefeuvre, F., 1988. Characterization of a homogeneous field turbulence from multipoint measurements. *Adv. Space Res.* 8 (9), 459–462.
- Pinçon, J.L., Lefeuvre, F., 1991. Local characterization of homogeneous turbulence in a space plasma from simultaneous measurements of field components at several points in space. *J. Geophys. Res.* 96, 1789–1802.
- Pinçon, J.L., Lefeuvre, F., 1992. The application of the generalized Capon method to the analysis of a turbulent field in space plasma: experimental constraints. *J. Atmos. Terr. Phys.* 54, 1237–1247.
- Pinçon, J.L., Motschmann, U., 1998. Multi-spacecraft filtering: general framework, Analysis Methods for Multi-Spacecraft Data, ISSI Scientific Report, SR-001, pp. 65–78.
- Robert, P., Roux, A., Harvey, C.C., Dunlop, M.W., Daly, P.W., Glassmeier, K.H., 1998. Tetrahedron geometric factors. Analysis Methods for Multi-Spacecraft Data, Scientific Report, International Space Science Institute, Bern, Switzerland, pp. 323–348.
- Sahraoui, F., Pinçon, J.L., Belmont, G., Rezeau, L., Cornilleau-Wehrin, N., Robert, P., Mellul, L., Bosqued, J.M., Balogh, A., Canu, P., Chanteur, G., 2003. ULF wave identification in the magnetosheath: the k -filtering technique applied to Cluster II data. *J. Geophys. Res.* 108, 1335–1354.
- Sahraoui, F., Belmont, G., Pinçon, J.L., Rezeau, L., Balogh, A., Robert, P., Cornilleau-Wehrin, N., 2004. Magnetic turbulent spectra in the magnetosheath: new insights (2004). *Ann. Geophys.* 22, 2283–2288.
- Sahraoui, F., Belmont, G., Rezeau, L., Cornilleau-Wehrin, N., Pinçon, J.L., Balogh, A., 2006. Anisotropic turbulent spectra in the terrestrial magnetosheath as seen by the cluster spacecraft. *Phys. Rev. Lett.* 96, 075002.
- Sahraoui, F., Goldstein, M.L., Robert, P., Khotyaintsev, Y.V., 2009. Evidence of a cascade and dissipation of solar-wind turbulence at the electron gyroscale. *Phys. Rev. Lett.* 102, 231102.
- Tjulin, A., Pinçon, J.L., Sahraoui, F., 2005. The k -filtering technique applied to wave electric and magnetic field measurements from the Cluster satellites. *J. Geophys. Res.* 110, A11224.